Published in *Solar Energy*, Volume 207, 1 September 2020, pp. 1045-1054,
https://doi.org/10.1016/j.solener.2020.07.043

Photovoltaic system monitoring for high latitude locations

Mari B. Ødgaard[a,b*], Heine Nygard Riise[b], Halvard Haug[a,b], Sabrina Sartori[a], Josefine H. Selj[a,b]

[a]Department of Technology Systems, University of Oslo
Gunnar Randers vei 19, 2007 Kjeller, Norway

[b] Renewable Energy Systems Department, Institute for Energy Technology
Instituttveien 18, 2007 Kjeller, Norway

*Corresponding author. E-mail: mari.ogaard@its.uio.no, Tel.: +47 976 356 08

Reliable monitoring of PV systems is essential to establish efficient maintenance routines that minimize the levelized cost of electricity. The existing solutions for affordable monitoring of commercial PV systems are however inadequate for climates where snow and highly varying weather result in unstable performance metrics. The aim of this work is to decrease this instability to enable more reliable monitoring solutions for PV systems installed in these climates.

Different performance metrics have been tested on Norwegian installations with a total installed capacity of 3.3 MW: i) comparison of specific yield, ii) temperature corrected performance ratio, and iii) power performance index based on both physical modelling and machine learning. The most influential effects leading to instability are identified as snow, low light, curtailment, and systematic irradiance differences over the system. The standard deviation of all the performance metrics is reduced when filters targeting these four effects are applied. Compared to general low irradiance or clear sky filtering, a greater reduction in the variation of the metrics is achieved, and more data remains in the useful dataset. The most suitable performance metrics are comparison of specific yield and performance index based on machine learning modelling.

The analysis highlights two paths to accomplish increased reliability of PV monitoring systems without increased hardware costs. First, better reliability can be achieved by selecting a suitable performance metric. Second, the variability of the performance metric can be reduced by utilizing filters that specifically target the origin of the variability instead of using standard literature thresholds.

Keywords: Photovoltaic systems; Monitoring; Filtering; Performance metric testing; Machine learning; High latitude climates

1. Introduction

1.1. PV system monitoring

With recent years' increased focus on operation and maintenance of photovoltaic (PV) systems related to its more important role in cost reduction (Klise et al., 2014; Whaley, 2016), numerous algorithms and performance metrics have been proposed to improve monitoring of PV installations (Daliento et al., 2017; Livera et al., 2019; Triki-Lahiani et al., 2018). The aim of these algorithms is to detect periods when the PV system is deviating from normal operation and identify faults. The existing solutions for affordable monitoring of commercial PV systems are however often inadequate for high latitude climates, as snow and highly varying weather result in unstable performance metrics.

PV system monitoring is typically based on a comparison between the production data directly acquired from the inverter and a yield target (Daliento et al., 2017). Examples of this is yield comparison of similar units (Skomedal et al., 2019), performance ratio (*PR*) with or without

Published in *Solar Energy*, Volume 207, 1 September 2020, pp. 1045-1054,
https://doi.org/10.1016/j.solener.2020.07.043

temperature correction (Dierauf et al., 2013; IEC, 2017; Woyte et al., 2014), and comparison with physical or data driven models of the system (Daliento et al., 2017). Due to the many parameters influencing PV energy generation (Fouad et al., 2017) which challenge accurate physical modelling, and the increasing amount of acquired data, machine learning have gained increased attention in PV system monitoring research in recent years (Daliento et al., 2017; Rodrigues et al., 2017; Triki-Lahiani et al., 2018).

Competitive solutions for automated monitoring of PV systems must have high sensitivity and fast detection, and at the same time minimize false alarms. This demands frequent and accurate performance estimation. Exact performance estimation is however challenging. Certain weather and irradiance conditions, seasonal soiling, shading, early system degradation, clipping or intentional curtailment, problems with data quality or lack of measurement availability (Jordan et al., 2017; Kurtz et al., 2013) can lead to errors or noise in the performance assessment. Noise will reduce the useful information that may be extracted from monitoring of commercial PV systems. It may lead to false alarms or conceal faults because the sensitivity of the fault detection is reduced. This causes challenges for implementation of generalized monitoring algorithms for commercial PV systems without extensive documentation and/or comprehensive instrumentation. This challenge is even greater for high latitude locations where seasonal soiling and variable irradiance conditions are especially prominent. Due to the drastic cost reductions for PV installations in recent years, the PV installation rate is rapidly increasing also in continental and subarctic climate zones. Consequently, the need for reliable monitoring solutions for these conditions is also increasing. For development of monitoring algorithms with high performance under difficult conditions, it is necessary to study the effect of data quality, snow cover, low light conditions and applied filtering more closely and subsequently investigate how the various monitoring methods need to be adjusted to different installation and weather conditions.

1.2. Data quality

In the PV monitoring standard IEC 61724-1, it is recommended to check for unphysical and missing values, and compare similar measurements to detect and remove erroneous PV system data caused by poor data quality (IEC, 2017). In the literature, more advanced methods are suggested, like assessment of expected relationships between measurements. Examples are calculations of the nominal operating cell temperature (NOCT) to evaluate irradiance and temperature measurements (Ransome, 2008) and relating temperature measurements to irradiance to detect detachment of module temperature sensors (Woyte et al., 2014). Øgaard et al. (2018) suggest comparison of irradiance measurements to modelled clear sky irradiance.

Dong et al. (2017) suggest to evaluate if fault characteristics are influenced by external factors, such as solar position, to detect variation caused by shading. For a location with a high share of clear days and direct light, this approach could be used to identify both deviations caused by shading and irradiance variations caused by differences in module tilt angles due to topography. For locations with larger share of diffuse light and cloudy weather, the correlation of these deviations with angle of incidence will be less clear.

1.3. Snow cover

Snow cover is a common seasonal soiling issue in high latitude locations, with high impact on PV system data. Handling snow covers in a monitoring system is important, as a full snow cover looks like an inverter breakdown, whereas a partial snow cover, leading to partial shading, can give power losses and changes in the maximum power point (Belhachat and Larbes, 2015) similar to serious PV module failures (Tsanakas et al., 2016). Snow cover is easy to identify by visual inspection, but it is not easily detected by an automated monitoring system without extra sensors. When analyzing historical data, snow cover is usually easily detected, as it can be characterized as transitory periods in

Published in *Solar Energy*, Volume 207, 1 September 2020, pp. 1045-1054,
https://doi.org/10.1016/j.solener.2020.07.043

the wintertime with no power production or low efficiency. In real time automated monitoring, it is challenging to predict the onset, duration and shading effect of the snow cover. To our knowledge, there are no reliable algorithm for detection of full and partial snow covers for real time monitoring presented in the literature.

1.4. Low light conditions

It is well known that low light conditions lead to noise in PV system analysis (Belluardo et al., 2015; Jordan et al., 2017; Reich et al., 2012). Typically, calculations of performance metrics result in high levels of noise in the morning and evening. Both the module and the inverter efficiencies are unstable under these conditions, as they are very sensitive to changes at low irradiance and power, and reflection losses are highly sensitive to changes in angle at high angle of incidence. Additionally, at lower irradiance levels a higher variation in module efficiencies could be anticipated, due to a potential variation in cell shunt resistance, as shown by Grunow et al. (2004). As discussed by Louwen et al. (2017), higher air mass, increased amount of diffuse irradiance and resulting spectral variation also impact efficiency, and hence increased instability at low light conditions. Reduced accuracy in irradiance measurements (Reise and Müller, 2018) and inverter measurements at lower irradiance/power levels, could give additional contributions to noise

1.5. Filtering

To reduce the uncertainty caused by noise at low irradiance conditions, filtering based on irradiance and clearness level is commonly used (Belluardo et al., 2015; Camus et al., 2018; Jordan et al., 2017; Reich et al., 2012; Silvestre et al., 2016). Moser et al. (2014) additionally filter out periods with high wind speed to ensure uniform temperature conditions, to further reduce uncertainties. To remove periods with clipping, Jordan et al. (2017) recommend to remove data where the power is >99 % of the maximum, and Meftah et al. (2019) suggest an upper irradiance limit.

Optimal filtering thresholds will depend on the system technology and the purpose of the analysis. Although methods to find optimal filtering thresholds to reduce noise in different datasets have been suggested, (Jordan and Kurtz, 2014; Skomedal et al., 2019) there are no standardized methods for data handling and filtering in PV system analysis. This is unfortunate, as recent studies on PV system performance loss (Curran et al., 2019) and degradation (Jordan et al., 2019; Jordan and Kurtz, 2014), show that different filtering and data handling methods can lead to differences in the loss estimate of more than one percentage point. This emphasizes a strong need for standardized methods. The effect of the applied filters will also depend on the specific dataset and operating environment of the PV system. In high latitude locations, typical filtering approaches like irradiance thresholds and clear sky filters can remove too much data rendering day-to-day monitoring difficult, while still not adequately reducing the noise (Øgaard et al., 2019).

1.6. Aim and approach

To identify areas of improvement of PV monitoring solutions in high latitude climates, we have tested four different PV system monitoring approaches (Y_f comparison, PR'_{STC}, *PPI* with physical and machine learning based modelling) using data from six commercial PV systems in Norway. The locations of the systems span various climate zones (Beck et al., 2018), but they are generally exposed to highly variable weather including long periods with low light conditions and snow. It is well known that snow (Andrews and Pearce, 2012; Marion et al., 2013) and low light conditions (Westbrook et al., 2012) constitute a challenge for accurate modelling of the PV energy generation. In the presented work, the challenges of PV system monitoring at high latitude locations have been evaluated, and the effect of applying tailored filters to remove specific conditions that generate noise is studied and compared to standard, more general filters used in PV monitoring. To enable detection of shading and irradiance differences caused by topography variations in locations with few clear sky days, we propose to use the statistical clear sky fitting algorithm suggested by Meyers et al. (2018). Based on

Published in *Solar Energy*, Volume 207, 1 September 2020, pp. 1045-1054,
https://doi.org/10.1016/j.solener.2020.07.043

this, improved methods for monitoring of PV systems in climates with highly variable weather and irradiance conditions is suggested.

2. Methodology

2.1. Dataset

The data in this study are taken from commercial PV systems on approximately flat roofed buildings, representing many of the larger systems in the Nordic countries. The modules are mounted with a tilt angle of ~10 ° in an east/west configuration. A such low tilt angle is not optimal for high latitude locations with respect to maximum production, but is typically used in installations on flat roof systems also in these types of locations to maximize roof coverage and to achieve a more even production distribution through the year. The exact orientation depends on the orientation of the building. Production data is collected from the inverters, and temperature and irradiance data are collected from the monitoring system of the installations. The sampling interval of the data logging is 5 minutes, and DC inverter data measured at maximum power point tracker level (MPPT) is used to increase granularity. The effective irradiance incident on the PV modules, i.e. the irradiance the modules can utilize (King et al., 2004; Stein and Farnung, 2017), is measured with a crystalline silicon reference cell in the plane of the PV modules. The irradiance measurements are controlled for shifts and degradation by comparison to modelled clear sky irradiance and the statistical clear sky method described in Section 2.3.1. Measurements of the reference cell temperature is used as an approximation for solar cell temperature. The cell temperature measurements are validated against module back sheet temperature measurements and thermography of the modules. The measurement uncertainty of the irradiance is ± 5 W/m^2 ± 2.5 % of measured value, and for the temperature it is 1 K. The inverters register curtailment and clipping events. Snow depth data is collected for each location from seNorge.no (NVE, 2019).

Relevant technical and geographical information about the systems are given in Table 1. For each location, the typical meteorological year (TMY) irradiance and ambient temperature is presented in Figure 1a and b, respectively. System 4 and the west oriented part of systems 1a and 1b lack temperature measurements and are excluded when temperature measurements are required to estimate performance metrics. As typical for systems at these coordinates, the yearly global horizontal irradiation is below 1000 kWh/m^2, most of the energy is generated at temperatures around 10-20 ℃, and the total share of diffuse light can reach 50 % (Imenes and Selj, 2017).

Table 1: Detailed information of the various PV plants investigated in this study. (#MPPTs = number of MPPTs in each direction)

Plant	Region	Coordinates [°N, °E]	Altitude [m a.s.l.]	Azimuth angles [°]	Installed capacity [kW]	# MPPTs	Time period
1a	Eastern Norway	59.59, 10.74	80	112/292	371	11	09-2014 – 09-2019
1b	Eastern Norway	59.59, 10.74	80	112/292	222	7	11-2016 – 09-2019
2	Eastern Norway	59.94, 10.87	126	128/308	471	15	12-2016 – 09-2019
3	Central Norway, inland	60.89, 10.92	158	122/302	421	12	06-2017 – 09-2019
4	Central Norway, coast	63.34, 10.37	154	111/291	931	7	07-2017 – 09-2019
5	Western Norway	60.40, 5.47	62	105/285	886	28	09-2017 – 09-2019

Published in *Solar Energy*, Volume 207, 1 September 2020, pp. 1045-1054,
https://doi.org/10.1016/j.solener.2020.07.043

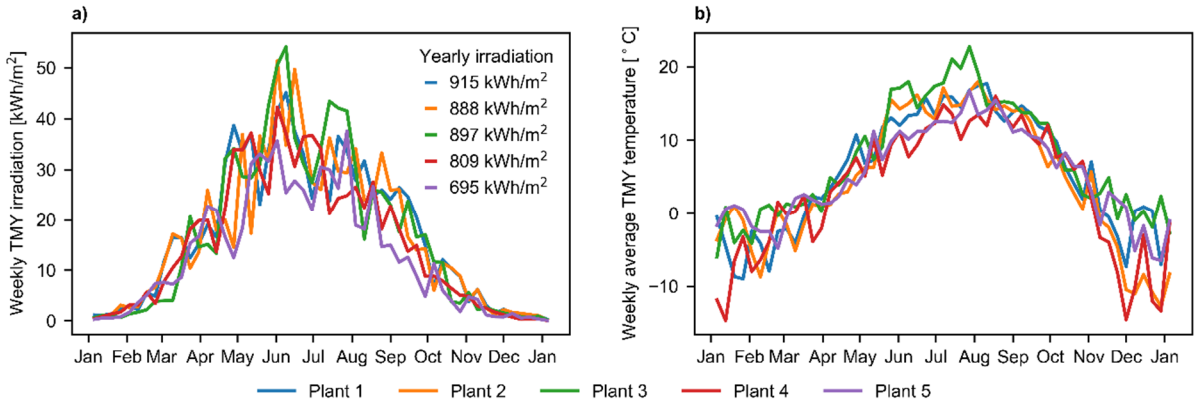

Figure 1: Yearly variation in a) weekly global horizontal TMY irradiation, and b) weekly average TMY ambient temperature. TMY data from PVGIS (Huld et al., 2012).

2.2. Performance metrics

Specific yield, performance ratio and power performance index are well known metrics to evaluate the performance of a PV system. The power performance index is the ratio of measured to modelled power, and both physical and statistical models can be used. In this work, the physical PVWatts model, the single diode model, and as an example of a machine learning model, a commonly used random forest regressor (Pedregosa et al., 2011) is selected.

To identify the conditions and effects which lead to the highest level of noise in the performance metrics, environmental and inverter parameters in the "noisy" time periods are evaluated. Sequentially, the identified noise-generating effects are removed from the dataset, and the procedure is repeated. Unphysical values are utilized to identify effects leading to bias in the performance metrics. Finally, a set of recommended filtering parameters is found. The effect of the suggested filters is quantified by the standard deviation of the metrics and by the percentage of remaining data points and energy. This will be compared to more general approaches: irradiance thresholding and clearness filtering. The filtering values from Jordan et al. (2017) (apparent clear sky conditions and irradiance threshold of 200 W/m^2) is used.

2.2.1. Yield comparison

The specific yield (Y_f) is the energy generated over a given time interval, divided by the rated power of the system (Woyte et al., 2014). For systems with multiple power measurements of units with identical configuration, comparing the specific yield of the different units allows for a monitoring system where weather conditions are inherently accounted for. The specific yield for each unit (MPPT measurement) in the system, $Y_{f\,DC}$, is compared to the median specific yield of all units, $\tilde{Y}_{f\,DC}$:

$$Y_{f\,rel} = Y_{f\,DC} \,/\, \tilde{Y}_{f\,DC}\,. \tag{1}$$

Using the median instead of the mean reduces the influence of outliers (*i.e.* anomalous MPPTs) in the comparison, reducing the risk of a biased result.

2.2.2. Temperature corrected performance ratio

To evaluate the yield for one unit over time, or to compare the yield of systems in different locations, the performance ratio corrected to standard test conditions (*STC*) temperature (PR'_{STC}) can be used (Daliento et al., 2017). PR'_{STC} is defined as the specific yield normalized to irradiance and temperature at STC (IEC, 2017), and is given by:

$$PR'_{STC} = \left(Y_{f\,DC} \,/ \left(1 + \gamma\left(T_{cell} - T_{STC}\right)\right)\right) / \left(G_{POA} \,/ G_{ref}\right). \tag{2}$$

Published in *Solar Energy*, Volume 207, 1 September 2020, pp. 1045-1054,
https://doi.org/10.1016/j.solener.2020.07.043

Here, G_{POA} is the measured plane of array irradiation in the same time interval as the specific yield, G_{ref} the reference irradiance 1000 W/m^2, T_{cell} is the estimated PV module temperature, T_{STC} is the reference temperature of 25 °C, and γ is the material dependent module power temperature coefficient. For the module technologies used at the five sites studied (different generations of mono- and multi-crystalline silicon) γ varies from -0.423 to -0.43 % / °C.

2.2.3. Power performance index

The power performance index (*PPI*) is a comparison between expected and measured power (IEC, 2017):

$$PPI = P_{\text{DC measured}} / P_{\text{DC expected}}. \quad (3)$$

The expected DC power output is simulated using both physical modelling and machine learning based modelling.

For the physical modelling, the single diode and the PVWatts models are used. The single diode model (Corkish et al., 2013) is commonly employed in PV modelling for monitoring (Daliento et al., 2017). The PVWatts DC power model (Dobos, 2014) is a simpler model with fewer module specific inputs. Similarly to PR'_{STC}, it uses G_{POA}, T_{cell}, γ and the nominal capacity (P_{DC0}) to model the expected DC power output:

$$P_{DC} = (G_{POA} / G_{ref}) \times P_{DC0}(1 + \gamma(T_{cell} - T_{STC})). \quad (4)$$

For the single diode model, module datasheet values is used as input to the System Advisor Model (SAM) (Blair et al., 2011) to estimate the diode ideality factor, light generated current, dark reverse saturation current, shunt resistance and series resistance at reference conditions, and the parameter for adjustment to temperature coefficient for short circuit current. These parameters are used as inputs to the CEC model described by Dobos (2012), together with the measured effective irradiance and cell temperature to estimate the photocurrent, saturation current, shunt resistance and thermal cell voltage under the different measured conditions. The expected power output for each module is estimated by solving the single diode equation based on the parameters estimated with the CEC model, as implemented in pvlib (F. Holmgren et al., 2018). An important difference between these models is that the single diode model includes the effect of the irradiance intensity on the PV efficiency. Figure 2 reports the values of the difference in modeled power using the two models against irradiance. The single diode model estimates a lower power value at low irradiance, and up to 1 % higher at irradiance levels around 500 W/m^2. This is in agreement with the results presented by Dobos et al. (2019). The total constant losses (L_{total}) for the physical models are estimated using the PVWatts system loss model (Dobos, 2014):

$$L_{\text{total}}(\%) = 100(1 - \Pi_i (1 - L_i)), \quad (5)$$

where L_i is the contribution from the individual loss mechanism (i) in percent. The modelled results are used for instant comparison with measured power values, and varying losses such as soiling, shading, snow and availability are therefore not included. The following loss mechanism values are used: Wiring = 2 %, connections = 0.5 % and light induced degradation = 1.5 %.

Published in *Solar Energy*, Volume 207, 1 September 2020, pp. 1045-1054,
https://doi.org/10.1016/j.solener.2020.07.043

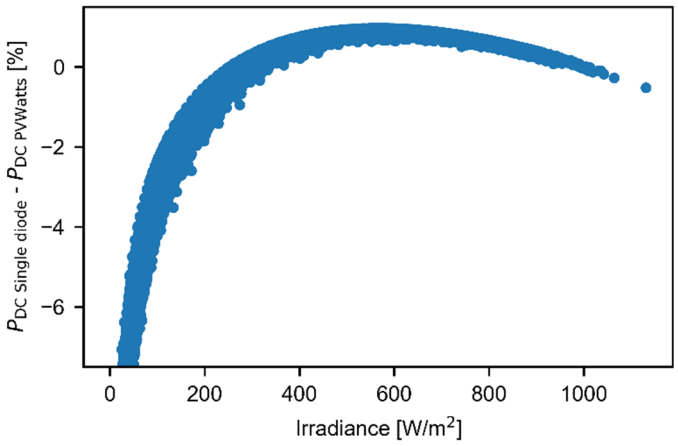

Figure 2: The irradiance dependency of the difference between the modeled power using the single diode model and the PVWatts model.

For the machine learning based model, a Random Forest (RF) regressor based on the sklearn library in Python (Pedregosa et al., 2011) is trained on historical irradiance and, when available, solar cell temperature data with power output per MPPT as model targets. According to Rodrigues et al. (2017), irradiance and temperature are the most common condition describing input features used in PV system modeling with machine learning. Only times with logged production data are used, and the data is split into a training set and a test set (80 % training set, 20 % test set). The regressor performance is evaluated on the test set using normalized root mean square error (*nRMSE*) as a metric:

$$nRMSE = \sqrt{\sum_{t=1}^{T}(\hat{y}_t - y_t)^2}\ /\ \bar{y}. \quad (6)$$

2.3. Methods used in filtering

2.3.1. Clear sky modelling and detection

The clear sky detection algorithm described by Reno and Hansen (2016) as implemented in pvlib python (F. Holmgren et al., 2018) is used for clear sky filtering. The pvlib python library is also used in the estimation of the POA clear sky irradiance used in the clear sky detection algorithm, and for the estimation of solar elevation, using the system configuration data as input. The clear sky curves for the irradiance sensors and each inverter string are also estimated with a more empirical approach: using the statistical clear sky fitting algorithm proposed by Meyers et al. (2018). With this algorithm, the clear sky current and irradiance for each day through the year are estimated based on the measured current and irradiance data. For the inverters, the current values are used instead of the power values in order to focus on the irradiance signal and exclude temperature effects. The fitted clear sky curves are used to detect systematic irradiance differences between the different inverters and the irradiance sensor. These differences are quantified by the ratio of the clear sky curve of the inverter to the median inverter clear sky curve or to the scaled irradiance curve. Additionally, the degradation application (Meyers et al., 2019) of the statistical clear sky fitting algorithm was used to control the irradiance measurements for drift.

2.3.2. Snow filtering

External snow depth measurements, often available from local weather measurements, are used for filtering out periods with snow on the modules. To ensure that periods with partial snow covers are removed from the data, all periods with snow on the ground (snow depth > 0 m) are removed. This

Published in *Solar Energy*, Volume 207, 1 September 2020, pp. 1045-1054,
https://doi.org/10.1016/j.solener.2020.07.043

removes more data than necessary as PV modules typically get snow free before the ground, but noise and potential false alarms are significantly reduced.

3. Results and discussion

3.1. Identification of conditions and effects leading to noise in performance evaluation

Based on the analysis procedure described in section 2.2., effects and conditions leading to noise, bias or difficulty in performance metric implementation are identified. The filters and filtering thresholds used to remove the different effects, and their impact on the dataset are presented and discussed in Section 3.2. The effects are categorized in the following categories: invalid data, data quality and availability, and unstable conditions. The invalid data category contains data where performance metric calculations yield illegitimate results. Effects leading to bias or systematic errors in the performance metrics are placed in the data quality and availability category. Noise generating situations are classified as unstable conditions.

3.1.1. Invalid data

The output considered as invalid in the performance evaluation, are zero output and an output wrongfully suggesting failures. Zero output is typically caused by downtime in monitoring measurements or communication. The main conditions giving false failures signatures in the production data, are snow and inverter induced power reduction. The power reduction is caused by both curtailment and inverter power clipping.

For monitoring algorithms based on yield comparisons on inverter/string level, full snow cover is not problematic as this will give the same behavior for all inverters/strings. Partial snow covers, however, may yield large relative differences due to (random) partial shading of the system, often with hard and uneven shading. These snow covers are difficult to predict, since they are influenced by several parameters and snow melting is stochastic by nature. This might be even more relevant for irradiance-based monitoring metrics: When the irradiance sensor is experiencing the same snow cover as the PV modules, the monitoring system will not report anomalous behavior. If the irradiance sensor is not covered, the resulting deviation between expected and actual production will lead to alarms. The PR'_{STC} values from one of the systems in a period of snow melting are presented in Figure 3, showing the large variations partial snow covers may inflict, especially between irradiance sensor and modules. On 21 March, both the PR'_{STC} and the irradiance are zero due to full snow cover. When the snow melts, the PR'_{STC} values increase until normal operation is reached, while the difference between the inverters only is large in the periods with substantial melting.

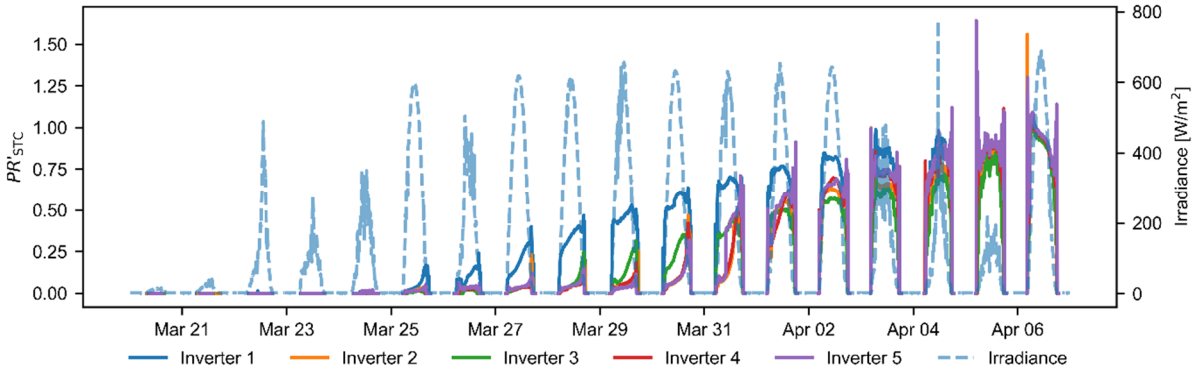

Figure 3: Measured irradiance and PR'_{STC} for different inverters for a system where the snow cover on the modules is melting during a time period of 18 days.

For performance evaluation based on machine learning, snow and curtailment are especially challenging. If not removed from the training data, these effects will perturb the correlations between

Published in *Solar Energy*, Volume 207, 1 September 2020, pp. 1045-1054,
https://doi.org/10.1016/j.solener.2020.07.043

irradiance, temperature and production. When the model attempts to accommodate these perturbations, the model might lose nuances at normal operation, potentially reducing the accuracy of the machine learning algorithm also in periods without snow or curtailment. As reported in Table 2, the *nRMSE* is indeed reduced when time periods with snow and curtailment are removed from the training and testing data set.

Table 2: The nRMSE of the machine learning model for the six systems for three different training datasets: raw data, dataset filtered for snow, and dataset filtered for snow and curtailment.

***nRMSE* [%]**	**1a**	**1b**	**2**	**3**	**4**	**5**
Raw data	12.8	15.1	21.8	44.2	26.6	24.3
Snow filter	8.8	12.5	18.9	33.7	20.5	16.7
Snow + curtailment filter	8.8	12.5	10.9	13.7	18.7	16.3

3.1.2. Data quality and availability

We find that systematic differences in irradiance level between different inverter strings, or between inverter strings and irradiance sensor, lead to solar position dependent errors for all the systems. This is especially prominent under clear conditions. The differences in irradiance are caused by shading and different tilt angles of the PV modules and/or the irradiance sensor. Such local and varying differences in irradiance affect the basis for accurate comparison for specific time periods during clear days. Both the variation in tilt of the modules and the sensor vary mainly with the roof topography. Minor errors in the installation of the irradiance sensor could also give similar results. Figure 4 shows how such local differences in irradiance impact the DC current of certain strings over a time period of one day. “System 1a” is a system where the modules in the strings of one the inverters have a slightly different tilt than the other strings. “System 1b” is a system with inhomogeneous shading conditions, where one inverter is experiencing more shading than the other inverters. For both systems, inverter 1 is an example of a normal inverter, and inverter 2 is the deviating inverter. The relative DC current of the inverters is also shown in Figure 4. For the deviating inverters in the two systems, a difference in the absolute and relative current compared to the other inverters depending on time of the day is clearly visible. This reflects the difference in irradiance of the inverters.

The estimated clear sky current signal based on the statistical clear sky algorithm for the inverters is plotted together with the measured clear sky current in Figure 4. We see that the measured and modelled values overlap well, except for the beginning and the end of the day. Hence, for most of the day, we can use these estimated curves to identify time periods where there are systematic irradiance differences between the modules. Figure 5 shows that even with large share of diffuse conditions, like at the tested systems, we get deviations through the year because of irradiance differences. The figure shows a boxplot with weekly values of relative current for one year for two normal inverters (top) and the two deviating inverters (bottom) in system 1a and 1b. Even though the weekly median relative current values of the deviating inverters are close to one in both cases, we see that the variation in the values is much larger than for the normal inverters. This implies that the deviations we see in Figure 4 are present through the year.

Comparison with estimated clear sky signal also enables identification of systematic irradiance differences between the inverter strings and the irradiance sensors, which give unstable results for the PR'_{STC} and the *PPI* based on physical modelling. PR'_{STC} and *PPI* are typically also impacted by other irradiance data sensor issues, like shifts, soiling and degradation. When the degradation application of the statistical clear sky algorithm was applied to the longer time series in the tested datasets however, no significant degradation in the irradiance sensors was detected in these cases. Temperature data quality issues may also have negative impact on these metrics. A general example of this, is that temperature measurements typically are point measurement and may not be representative for the whole system. Physical system modelling is additionally influenced by availability of system data

Published in *Solar Energy*, Volume 207, 1 September 2020, pp. 1045-1054,
https://doi.org/10.1016/j.solener.2020.07.043

challenging accurate estimations of balance of systems (BOS) losses, i.e. constant losses in cables and connectors, or the production dependent losses of the inverter. These losses vary between installations due to different configurations. The machine learning model automatically takes these losses into account, and is to a larger degree able to handle the effect of non-representative temperature measurements. Degradation in the irradiance sensor will however also impact the quality of the machine learning based model. Immunity to sensor data quality issues are one of the strengths of monitoring systems based on comparison of specific yield.

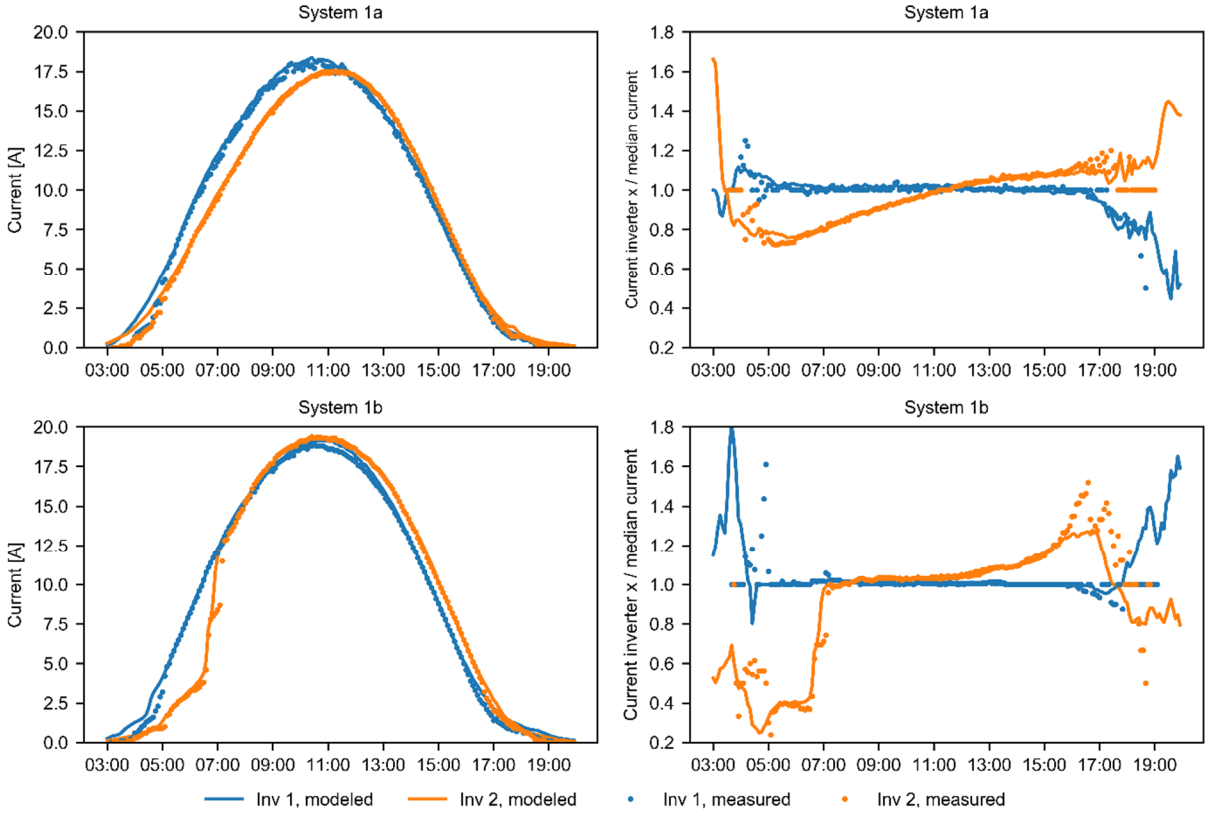

Figure 4: Absolute (left) and relative (right) clear sky current values for one day, representing the clear sky irradiance for different inverter strings, for a system where one string has modules with a slightly different tilt than the rest of the strings (1a), and a system where one string is differently shaded than the other two (1b). Modeled (straight line) and measured (dots) values.

Published in *Solar Energy*, Volume 207, 1 September 2020, pp. 1045-1054,
https://doi.org/10.1016/j.solener.2020.07.043

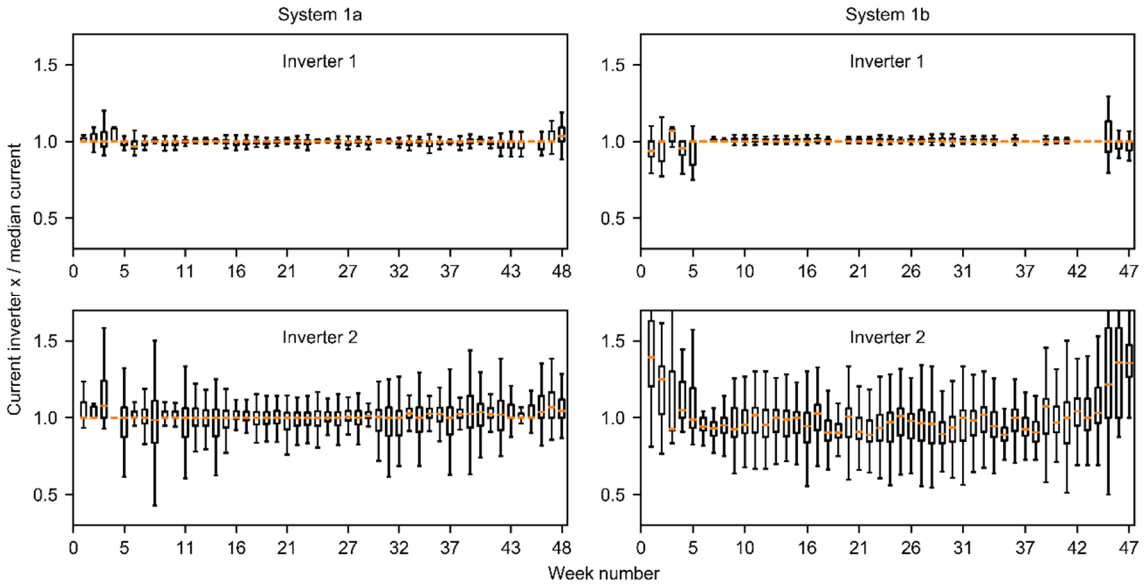

Figure 5: Boxplot of weekly relative current values for one year for two normal inverters in system 1a and 1b (top) compared to the two deviating inverters in the same systems (bottom). The box extends from the first to the third quartile values of the data, with a line on the median. The whiskers extend to maximum 1.5 multiplied the interquartile range, and outliers are not included.

3.1.3. Unstable periods

As previously mentioned, it is well known that low light conditions lead to noise in PV system analysis. The resulting noise in the morning and evening is normally filtered out by removing low irradiance periods. The noise in this period is however not only due to low irradiance: high angles of incidence may cause additional instability in this period.

Figure 6, shows how high (>0.1, noisy data) and low (<0.1) standard deviation in the specific yield comparisons of system 1a correlate to irradiance and solar elevation angle. We use solar elevation as an indicator of angle of incidence instead of using the actual angle of incidence. Calculating the angle of incidence explicitly, and using it as a basis for filtering, requires accurate definitions in the system configuration input data, specifically tilt and azimuth angles. The histograms show all the data except snow periods, with the scatterplot showing a randomly selected sample of these data. It is clear that a typical low irradiance filter (<200 W/m^2) would remove data points that do not have particularly high standard deviation. Replacing in this case the 200 W/m^2 low irradiance filter with a 50 W/m^2 filter *and* a solar elevation angle threshold of 20 ° will remove most of the noisy data, while a larger set of useful data remains. Therefore, a more detailed filtering procedure, specifically removing the conditions leading to instability, can lead to an increase in data points without increasing the noise. The trend is representative for all the tested systems, although there are some differences in the optimal filtering thresholds. The differences can be partially explained by inverter sizing. The inverter efficiency is not directly related to irradiance, but with power and inverter capacity ratio, hence, undersized inverters would reach a stable efficiency at lower irradiance conditions than oversized inverters.

Published in *Solar Energy*, Volume 207, 1 September 2020, pp. 1045-1054,
https://doi.org/10.1016/j.solener.2020.07.043

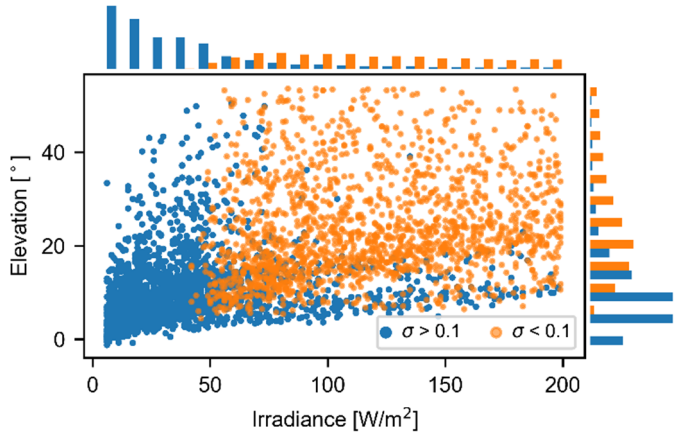

Figure 6: Comparison of irradiance and solar elevation conditions for time stamps where there is a standard deviation in the yield comparison in system 1a of >0.1 and <0.1. All data are shown in the histograms, a randomly selected sample of the data is shown in the scatterplot.

Other types of conditions observed to give unstable performance metrics in the datasets, are fast and large changes in irradiance transitions caused by moving clouds. With rapidly changing irradiance, the efficiency of the maximum power point tracker (MPPT) may decrease (Sanchis et al., 2007), or the moving clouds may lead to uneven shading and mismatch in the system (Lappalainen and Valkealahti, 2017), resulting in unpredictable losses. These losses will however last for very short time periods.

3.2. Impact of the identified effects on the performance evaluation methods

An overview of all the identified effects which generate noise or errors in the performance estimations discussed in Section 3.1. is given in Table 3. A qualitative assessment of their influence on the different performance metrics is provided.

Table 3: Overview of the different identified noise generating effects and their influence on different performance metrics.

	Challenge	**Yield comparison**	***PR'*$_{STC}$**	***PPI*: Physical modelling**	***PPI*: Statistical modelling**
Invalid data	Snow	Noise if partial snow cover	Low/zero values, potentially over longer time periods (weeks)		
	Clipping, Curtailment	Noise if not equal for all inverters	Low values, potentially for multiple hours a day		
Data quality and availability	Constant system losses	Inaccurate estimations if not equal for all inverters		Estimation for every system necessary	-
	Systematic differences in irradiance	Inaccurate estimation if differences between inverters	Inaccurate estimation if differences between inverters and irradiance sensor		-
	Degradation in irradiance data	-	Bias/shifts depending on degradation type		
Unstable periods	Low light conditions	Noise			
	Rapid, large irradiance changes	Noise, short time period			

The impact of consecutively filtering out the effects with largest contribution to noise (snow, low light conditions, curtailment and periods with systematic differences in irradiance levels) on the standard deviation of the performance metrics is presented in Figure 7. Rapid irradiance changes give less

Published in *Solar Energy*, Volume 207, 1 September 2020, pp. 1045-1054,
https://doi.org/10.1016/j.solener.2020.07.043

contribution to noise, because it only affects short time periods. The constant system losses introduce no variability, but a bias in the metrics, especially for the *PPI* based on physical modelling. This can be corrected for by learning from the data, but not filtered out. The filters presented in Table 4 are used for removing data, based on the findings presented in previous sections. For the irradiance difference filtering, a ± 2.5 % difference between the inverters clear sky current and the clear sky median inverter current or the scaled clear sky measured irradiance is set. As the filtering is performed consecutively and the parameters are not independent, this does not quantify the noise generation of the different parameters. The variation in all the metrics is significantly reduced when the filters for removing snow periods and low light conditions are applied. The performance index based on machine learning modelling especially experienced large variations at low light conditions due to frequent underestimation of the power in these periods. The results are compared to more standard filtering approaches based on irradiance and clearness level in Table 5. We see that a filter for low light conditions based on the parameters in Table 4 in combination with a snow filter gives lower variation and more data than a standard irradiance or clear sky filter. The clear sky filter especially removes large amounts of data under the given climatic conditions.

Table 4: Filters used in the standard filtering approach and the system specific filtering approach.

Parameter	**Filters**
Standard	
Irradiance	$G_{POA} > 200$ W/m^2
Clear sky	pvlib detect_clearsky
System specific	
Snow	Snow depth > 0 m
Irradiance difference	$I_{\text{Clear sky, Inverter}} / I_{\text{Clear sky, reference}} < \pm 0.025$
Low light	
Irradiance	$G_{POA} > 50$ W/m^2
Solar elevation	Solar elevation angle > 20 ^{o}

The variations in the metrics are further reduced by adding filters for systematic irradiance differences, curtailment and inverter clipping. Some of the systems had poor tilt angle match between irradiance sensor and the modules, resulting in removal of a large share of the data when the irradiance difference filter is applied for the irradiance-based performance metrics. Only the machine learning model can handle the systematic irradiance differences caused by shading and the difference in tilt between different PV modules and the irradiance sensor. Figure 7 shows that the irradiance difference filter does not have the same impact on reduction of the standard deviation for the machine learning based *PPI* as for the other performance metrics. Traditional low irradiance filtering or clear sky filtering is not sufficient in situations of irradiance differences and curtailment. In some cases, irradiance differences caused by shading and topography variations will be most prominent at low irradiance levels, and inadvertently be removed at low irradiance filtering. These effects will however be more prominent at clear sky, and curtailment and inverter clipping are more likely to occur at high energy generation and irradiance.

The yearly PR'_{STC} values using data filtered for irradiance difference vary from 0.68 to 0.93. In the winter months we see significant losses for all the systems due to both snow and low light condition, and in the summer some of the systems have significant curtailment losses.

Published in *Solar Energy*, Volume 207, 1 September 2020, pp. 1045-1054,
https://doi.org/10.1016/j.solener.2020.07.043

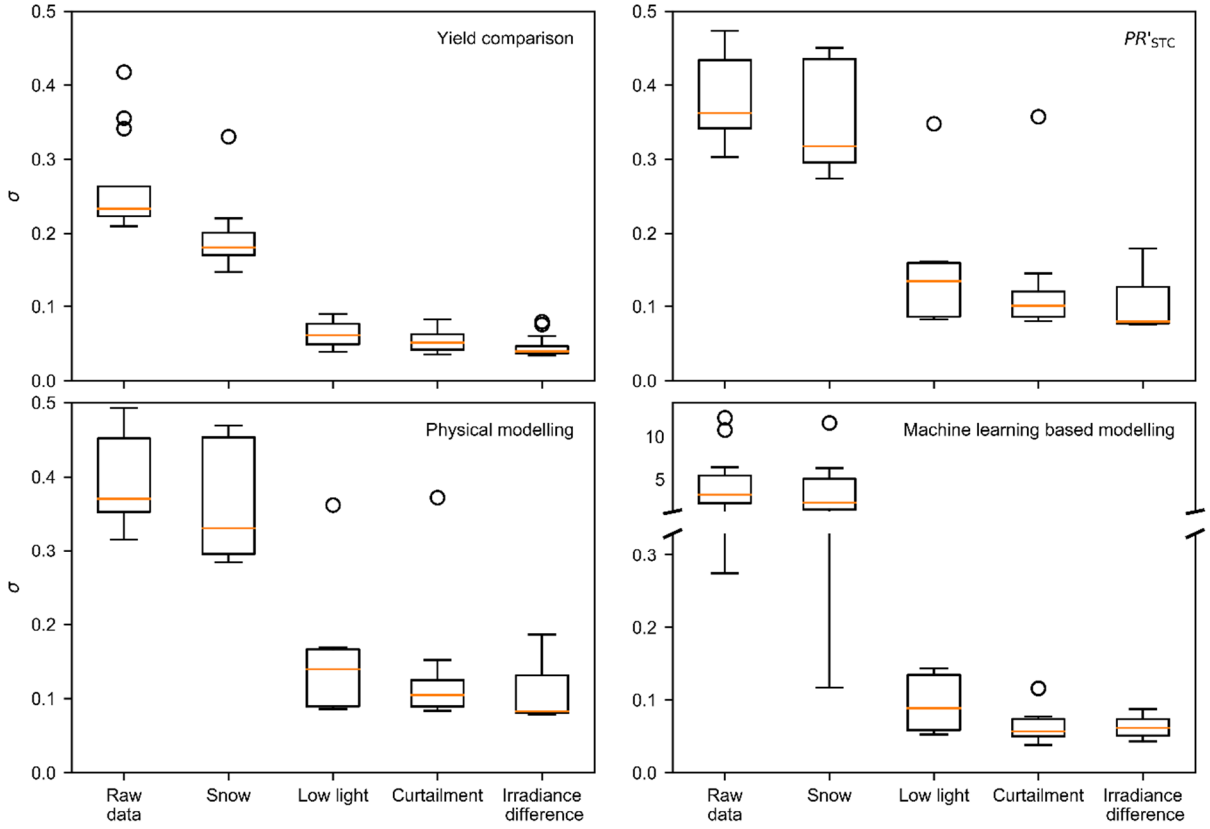

Figure 7: Variation in median standard deviation in different performance metrics for the different MPPTs in all the systems, showing the effect when different filters (snow, low light conditions, curtailment, irradiance difference) is consecutively applied. The box extends from the first to the third quartile values of the data, with a line on the median. The whiskers extend to maximum 1.5 multiplied the interquartile range, and outliers are shown as circles.

Table 5: Median standard deviation and share of remaining data points and energy for the system specific filtering (consecutively applied) compared to more standard filtering strategies: 200 W/m^2 irradiance cut off and clear sky filtering. For the irradiance difference filter there is especially large system variations in how much of the data that are removed.

Filters	***Median standard deviation***					***Median***	
	$Y_{f\,rel}$	***PR'$_{STC}$***	***PPI:* PVWatts**	***PPI:* Single diode**	***PPI:* Machine learning**	**Remaining data points**	**Remaining energy**
None (raw data)	0.23	0.36	0.38	0.39	3.44	100 %	100 %
Standard filtering							
Irradiance >200 W/m^2	0.14	0.17	0.18	0.18	0.17	34 %	76 %
Clear sky	0.22	0.36	0.38	0.38	0.45	14 %	20 %
Specific filtering							
Snow	0.18	0.32	0.33	0.34	2.57	94 %	98 %
Low light	0.06	0.13	0.14	0.14	0.09	47 %	83 %
Curtailment	0.05	0.10	0.10	0.11	0.06	43 %	69 %
Irradiance difference	0.04	0.08	0.08	0.08	0.06	-	3- 58 %

4. Conclusions

Five effects that reduce the stability of the monitoring systems are identified: i) Snow, ii) curtailment & clipping, iii) systematic irradiance differences over the system, iv) low light conditions and v) rapid changes in irradiance. The four first are most influential, as they might impact longer time periods. The standard deviation of all the performance metrics are significantly reduced when narrowly targeted filters for these four effects are applied. Compared to general low irradiance or clear sky

Published in *Solar Energy*, Volume 207, 1 September 2020, pp. 1045-1054,
https://doi.org/10.1016/j.solener.2020.07.043

filtering, the reduction in standard deviation of the metrics is greater, while more data remains in the useful dataset. Difficulty in estimating the constant system losses for different installation and sensor data quality issues may also introduce bias in some of the performance metrics.

More efficient filtering of low light conditions can be achieved by filtering with respect to both solar elevation and irradiance to directly address the issues leading to noise. To detect periods with systematic differences in irradiance between different units, statistical clear sky fitting can be employed.

The solutions of the discussed challenges and the specific filtering approaches are relevant for analysis and monitoring of most PV systems, when recognizing different effects in the data and efficient filtering is necessary. Automatic detection of periods with irradiance differences caused by e.g. shading or topography is particularly important for robust PV system analysis. The suggested methods will however be especially important for systems at higher latitudes exposed to more unstable conditions.

Filtered values of specific yield comparison and power performance index based on machine learning modelling yielded best results in terms of a stable metric. *PPI* based on physical modeling gives inaccurate results because of insufficient input data to estimate losses and dependency of accurate irradiance measurements. Machine learning based modeling handled both these challenges and periods with systematic differences in irradiance more efficiently, showing that data driven methods might be particularly suitable for challenging weather conditions and systems with lower grade of uniformity.

The analysis highlights two paths to accomplish increased reliability of PV monitoring systems without increased hardware costs. First, better reliability can be achieved by evaluating the availability and the quality of the input data, then based on this choose a suitable performance metric. Second, the variability of the chosen performance metric can be reduced by utilizing filters that specifically target the origin of the variability instead of using typical literature thresholds. As this analysis focuses on challenges and limitations met in monitoring of commercial PV systems, implementing the suggested solutions in monitoring software would improve the performance analysis and fault detection in the system. This could increase the PR and reduce the levelized cost of electricity.

Acknowledgments

The authors acknowledge funding from the Innovation project number 803801 (Autonomous monitoring, control and protection of renewable energy infrastructure).

References

Andrews, R.W., Pearce, J.M., 2012. Prediction of energy effects on photovoltaic systems due to snowfall events, in: 2012 38th IEEE Photovoltaic Specialists Conference. IEEE, pp. 3386–3391. https://doi.org/10.1109/PVSC.2012.6318297

Beck, H.E., Zimmermann, N.E., McVicar, T.R., Vergopolan, N., Berg, A., Wood, E.F., 2018. Present and future köppen-geiger climate classification maps at 1-km resolution. Sci. Data 5. https://doi.org/10.1038/sdata.2018.214

Belhachat, F., Larbes, C., 2015. Modeling, analysis and comparison of solar photovoltaic array configurations under partial shading conditions. Sol. Energy 120, 399–418. https://doi.org/10.1016/j.solener.2015.07.039

Published in *Solar Energy*, Volume 207, 1 September 2020, pp. 1045-1054,
https://doi.org/10.1016/j.solener.2020.07.043

Belluardo, G., Ingenhoven, P., Sparber, W., Wagner, J., Weihs, P., Moser, D., 2015. Novel method for the improvement in the evaluation of outdoor performance loss rate in different PV technologies and comparison with two other methods. Sol. Energy 117, 139–152. https://doi.org/10.1016/j.solener.2015.04.030

Blair, N., Dobos, A.P., Freeman, J., Neises, T., Wagner, M., Ferguson, T., Janzou, S., 2011. System advisor model, sam 2014.1. 14: General description, No. NREL/TP-6A20-61019. Golden, CO (United States).

Camus, C., Hüttner, M., Lassahn, D., Kurz, C., Hauch, J., Brabec, C.J., 2018. Data-filtering-dependent variability of long-term degradation rates of MW-scale photovoltaic power plants from "non-ideal" monitoring and weather data, in: Proceedings of the 35th European Photovoltaic Solar Energy Conference and Exhibition. pp. 2069–2074. https://doi.org/10.3130/aijsaxx.152.0_69

Corkish, R., Green, M.A., Watt, M.E., Wenham, S.R., 2013. Applied Photovoltaics. Routledge. https://doi.org/10.4324/9781849770491

Curran, A.J., Jones, C.B., Lindig, S., Stein, J., Moser, D., French, R.H., 2019. Performance loss rate consistency and uncertainty across multiple methods and filtering criteria, in: 2019 IEEE 46th Photovoltaic Specialists Conference. IEEE, pp. 1328–1334.

Daliento, S., Chouder, A., Guerriero, P., Pavan, A.M., Mellit, A., Moeini, R., Tricoli, P., 2017. Monitoring, diagnosis, and power forecasting for photovoltaic fields: A review. Int. J. Photoenergy 2017. https://doi.org/10.1155/2017/1356851

Dierauf, T., Growitz, A., Kurtz, S., Hansen, C., 2013. Weather-corrected performance ratio, No. NREL/TP-5200-57991. Golden, CO (United States).

Dobos, A.P., 2014. PVWatts Version 5 Manual, No. NREL/TP-6A20-62641. Golden, CO (United States). https://doi.org/10.2172/1158421

Dobos, A.P., 2012. An improved coefficient calculator for the California energy commission 6 parameter photovoltaic module model. J. Sol. Energy Eng. 134. https://doi.org/10.1115/1.4005759

Dobos, A.P., Freeman, J.M., Blair, N.J., 2019. Improvements to PVWatts for Fixed and One-Axis Tracking Systems, No. NREL/CP-6A20-74097. Golden, CO (United States). https://doi.org/10.1109/pvsc40753.2019.8981312

Dong, A., Zhao, Y., Liu, X., Shang, L., Liu, Q., Kang, D., 2017. Fault diagnosis and classification in photovoltaic systems using scada data, in: 2017 International Conference on Sensing, Diagnostics, Prognostics, and Control. IEEE, pp. 117–122. https://doi.org/10.1109/SDPC.2017.31

F. Holmgren, W., W. Hansen, C., A. Mikofski, M., 2018. pvlib python: a python package for modeling solar energy systems. J. Open Source Softw. 3, 884. https://doi.org/10.21105/joss.00884

Fouad, M.M., Shihata, L.A., Morgan, E.S.I., 2017. An integrated review of factors influencing the performance of photovoltaic panels. Renew. Sustain. Energy Rev. 80, 1499–1511. https://doi.org/10.1016/j.rser.2017.05.141

Grunow, P., Lust, S., Sauter, D., Hoffmann, V., Podlowski, L., 2004. Weak light performance and annual yields of PV modules and systems as result of the basic parameter set of industrial solar cells, in: Proceedings of the 19th European Photovoltaic Solar Energy Conference. pp. 2190–2193.

Huld, T., Müller, R., Gambardella, A., 2012. A new solar radiation database for estimating PV performance in Europe and Africa. Sol. Energy 86, 1803–1815.

Published in *Solar Energy*, Volume 207, 1 September 2020, pp. 1045-1054,
https://doi.org/10.1016/j.solener.2020.07.043

https://doi.org/10.1016/j.solener.2012.03.006

IEC, 2017. Photovoltaic system Performance - Part 1: Monitoring (IEC 61724-1.0, 2017-03). Geneva, Switerland.

Imenes, A.G., Selj, J., 2017. Irradiance and temperature distributions at high latitudes: Design implications for photovoltaic systems, in: 2017 IEEE 44th Photovoltaic Specialist Conference. IEEE, pp. 619–625. https://doi.org/10.1109/PVSC.2017.8366376

Jordan, D.C., Deline, C., Deceglie, M.G., Nag, A., Kimball, G.M., Shinn, A.B., John, J.J., Alnuaimi, A.A., Elnosh, A.B.A., Luo, W., Jain, A., Saleh, M.U., von Korff, H., Hu, Y., Jaubert, J.-N., Mavromatakis, F., 2019. Reducing interanalyst variability in photovoltaic degradation rate assessments. IEEE J. Photovoltaics 10, 206–212. https://doi.org/10.1109/jphotov.2019.2945191

Jordan, D.C., Deline, C., Kurtz, S.R., Kimball, G.M., Anderson, M., 2017. Robust PV degradation methodology and application. IEEE J. Photovoltaics 8, 525–531. https://doi.org/10.1109/JPHOTOV.2017.2779779

Jordan, D.C., Kurtz, S.R., 2014. The dark horse of evaluating long-term field performance-Data filtering. IEEE J. Photovoltaics 4, 317–323. https://doi.org/10.1109/JPHOTOV.2013.2282741

King, D.L., Kratochvil, J.A., Boyson, W.E., 2004. Photovoltaic array performance model, No. SAND2004-3535. https://doi.org/10.2172/919131

Klise, G.T., Balfour, J.R., Keating, T.J., 2014. Solar PV O&M standards and best practices - existing gaps and improvement efforts, No. SAND2014-19432. Albuquerque, NM (United States).

Kurtz, S., Newmiller, J., Kimber, A., Flottemesch, R., Riley, E., Dierauf, T., McKee, J., Krishnani, P., 2013. Analysis of photovoltaic system energy performance evaluation method, No. NREL/TP-5200-60628. Golden, CO (United States).

Lappalainen, K., Valkealahti, S., 2017. Output power variation of different PV array configurations during irradiance transitions caused by moving clouds. Appl. Energy 190, 902–910. https://doi.org/10.1016/j.apenergy.2017.01.013

Livera, A., Theristis, M., Makrides, G., Georghiou, G.E., 2019. Recent advances in failure diagnosis techniques based on performance data analysis for grid-connected photovoltaic systems. Renew. Energy 133, 126–143. https://doi.org/10.1016/j.renene.2018.09.101

Louwen, A., de Waal, A.C., Schropp, R.E.I., Faaij, A.P.C., van Sark, W., 2017. Comprehensive characterisation and analysis of PV module performance under real operating conditions. Prog. Photovoltaics 25, 218–232. https://doi.org/10.1002/pip

Marion, B., Schaefer, R., Caine, H., Sanchez, G., 2013. Measured and modeled photovoltaic system energy losses from snow for Colorado and Wisconsin locations. Sol. Energy 97, 112–121. https://doi.org/10.1016/j.solener.2013.07.029

Meftah, M., Lajoie-Mazenc, E., Van Iseghem, M., Perrin, R., Boublil, D., Radouane, K., 2019. A less environment-sensitive and data-based approach to evaluate the performance loss rate of PV power plants, in: Proceedings of the 36th European Photovoltaic Solar Energy Conference and Exhibition. pp. 1554–1559. https://doi.org/10.1017/CBO9781107415324.004

Meyers, B., Deceglie, M., Deline, C., Jordan, D., 2019. Signal Processing on PV Time-Series Data : Robust Degradation Analysis without Physical Models. 46th IEEE Photovolt. Spec. Conf. PP, 1–8. https://doi.org/10.1109/JPHOTOV.2019.2957646

Meyers, B., Tabone, M., Kara, E.C., 2018. Statistical Clear Sky Fitting Algorithm, in: 2018 45th IEEE Photovoltaic Specialist Conference. IEEE.

Moser, D., Pichler, M., Nikolaeva-Dimitrova, M., 2014. Filtering procedures for reliable outdoor temperature coefficients in different photovoltaic technologies. J. Sol. Energy Eng. 136.

Published in *Solar Energy*, Volume 207, 1 September 2020, pp. 1045-1054,
https://doi.org/10.1016/j.solener.2020.07.043

https://doi.org/10.1115/1.4024931

NVE, 2019. seNorge [WWW Document]. URL www.senorge.no (accessed 9.1.19).

Øgaard, M.B., Haug, H., Selj, J., 2018. Methods for quality control of monitoring data from commercial PV systems, in: Proceedings of the 35th European Photovoltaic Solar Energy Conference and Exhibition. pp. 2083–2088. https://doi.org/10.4229/35thEUPVSEC20182018-6DV.1.53

Øgaard, M.B., Skomedal, Å., Selj, J.H., 2019. Performance Evaluation of Monitoring Algorithms for Photovoltaic Systems, in: Proceedings of the 36th European Photovoltaic Solar Energy Conference and Exhibition. pp. 1632–1636.

Pedregosa, F., Weiss, R., Brucher, M., Varoquaux, G., Gramfort, A., Michel, V., Thirion, B., Grisel, O., Blondel, M., Prettenhofer, P., Weiss, R., Dubourg, V., Vanderplas, J., Passos, A., Cournapeau, D., Brucher, M., Perrot, M., Duchesnay, É., 2011. Scikit-learn: Machine Learning in Python. J. Mach. Learn. Res. 12, 2825–2830.

Ransome, S., 2008. Array performance analysis using imperfect or incomplete input data, in: Proceedings of the 23rd European Photovoltaic Solar Energy Conference and Exhibition. pp. 3187–3191.

Reich, N.H., Goebel, A., Dirnberger, D., Kiefer, K., 2012. System performance analysis and estimation of degradation rates based on 500 years of monitoring data, in: 2012 38th IEEE Photovoltaic Specialists Conference. IEEE, pp. 1551–1554. https://doi.org/10.1109/PVSC.2012.6317890

Reise, C., Müller, B., 2018. Uncertainties in PV system yield predictions and assessments, Report IEA-PVPS T13-12.

Reno, M.J., Hansen, C.W., 2016. Identification of periods of clear sky irradiance in time series of GHI measurements. Renew. Energy 90, 520–531. https://doi.org/10.1016/j.renene.2015.12.031

Rodrigues, S., Ramos, H.G., Morgado-Dias, F., 2017. Machine learning in PV fault detection, diagnostics and prognostics: A review, in: 2017 44th IEEE Photovoltaic Specialist Conference. IEEE, pp. 3178–3183. https://doi.org/10.1109/PVSC.2017.8366581

Sanchis, P., López, J., Ursúa, A., Gubía, E., Marroyo, L., 2007. On the testing, characterization, and evaluation of PV inverters and dynamic MPPT performance under real varying operating conditions. Prog. Photovoltaics Res. Appl. 15, 541–556. https://doi.org/10.1002/pip

Silvestre, S., Mora-López, L., Kichou, S., Sánchez-Pacheco, F., Dominguez-Pumar, M., 2016. Remote supervision and fault detection on OPC monitored PV systems. Sol. Energy 137, 424–433. https://doi.org/10.1016/j.solener.2016.08.030

Skomedal, Å., Øgaard, M.B., Selj, J.H., Haug, H., Marstein, E.S., 2019. General, robust and scalable methods for string level monitoring in utility scale PV systems, in: Proceedings of the 36th European Photovoltaic Solar Energy Conference and Exhibition. pp. 1283–1287.

Stein, J.S., Farnung, B., 2017. PV Performance Modeling Methods and Practices Results from the 4th PV Performance Modeling Collaborative Workshop, Report IEA-PVPS T13-06:201.

Triki-Lahiani, A., Abdelghani, A.B.-B., Slama-Belkhodja, I., 2018. Fault detection and monitoring systems for photovoltaic installations: A review. Renew. Sustain. Energy Rev. 82, 2680–2692. https://doi.org/10.1016/j.rser.2017.09.101

Tsanakas, J.A., Ha, L., Buerhop, C., 2016. Faults and infrared thermographic diagnosis in operating c-Si photovoltaic modules: A review of research and future challenges. Renew. Sustain. Energy Rev. 62, 695–709. https://doi.org/10.1016/j.rser.2016.04.079

Westbrook, O.W., Copanas, B.H., Collins, F.D., 2012. New approaches for characterizing

Published in *Solar Energy*, Volume 207, 1 September 2020, pp. 1045-1054,
https://doi.org/10.1016/j.solener.2020.07.043

photovoltaic system performance, in: 2012 38th IEEE Photovoltaic Specialists Conference. IEEE, pp. 1529–1534. https://doi.org/10.1109/PVSC.2012.6317886

Whaley, C., 2016. Best practices in photovoltaic system operations and maintenance, No. NREL/TP-7A40-67553. Golden, CO (United States).

Woyte, A., Richter, M., Moser, D., Green, M., Mau, S., Beyer, H.G., 2014. Analytical monitoring of grid-connected photovoltaic systems, Report IEA-PVPS T13-03. https://doi.org/10.13140/2.1.1133.6481